

Coordinated Activities of Multiple Myc-Dependent and Myc-Independent Biosynthetic Pathways in Hepatoblastoma

Huabo Wang¹, Jie Lu¹, Lia R. Edmunds¹, Sucheta Kulkarni¹, James Dolezal¹, Junyan Tao², Sarangarajan Ranganathan³, Laura Jackson⁴, Marc Fromherz¹, Donna Beer Stolz⁵, Radha Uppala⁶, Sivakama Bharathi⁶, Satdarshan P. Monga^{2,7}, Eric S. Goetzman⁶, Edward V. Prochownik^{1,8,9,*}

1. The Division of Hematology/Oncology, Children's Hospital of Pittsburgh of UPMC, Pittsburgh, PA;
2. The Department of Pathology, The University of Pittsburgh Medical Center, Pittsburgh PA;
3. The Department of Pathology, Children's Hospital of Pittsburgh of UPMC;
4. The Division of Neonatology, Children's Hospital of Pittsburgh of UPMC, Pittsburgh, PA;
5. The Department of Cell Biology, The University of Pittsburgh Medical Center, Pittsburgh PA;
6. The Division of Medical Genetics, Children's Hospital of Pittsburgh of UPMC;
7. The Division of Gastroenterology, Hepatology and Nutrition, Department of Medicine, The University of Pittsburgh Medical Center;
8. The Department of Microbiology and Molecular Genetics, The University of Pittsburgh Medical Center;
9. The University of Pittsburgh Cancer Institute

Running Title: *Coordinated Biosynthetic Pathways in Hepatoblastoma*

*Address correspondence to: Edward V. Prochownik, MD, PhD, Division of Hematology/Oncology, Children's Hospital of Pittsburgh of UPMC, Rangos Research Center, Room 5124, 4401 Penn Ave., Pittsburgh, PA 15224, Email: procev@chp.edu, Phone: 412-692-6795; Fax 412-692-5228

Key words: β-catenin, YAP, metabolism, oxidative phosphorylation, hepatocellular carcinoma

SUPPLEMENTAL FIGURE LEGENDS

Supplemental Figure S1. Expression of potential Myc surrogates in WT and KO hepatocytes and HBs. *A*, Transcript levels for the indicated genes was obtained from RNA seq data performed on WT and KO HBs. *B*, Immuno-blotting for the indicated proteins of WT and KO livers (L) and HBs (T)

Supplemental Figure S2. Structure and function of ETC complexes in livers and HBs. *A*, Top panel: Representative BNGE of ETC complexes from paired WT and KO livers (L) and HBs (T) stained with Coomassie Blue. Bottom panels: Representative examples of *in situ* enzymatic activities for ETC complexes I, III, IV and V. SC=super-complexes composed of varying stoichiometries of Complexes I, II and IV. *B*, Quantification of relative specific activities of *in situ* enzymatic activities after normalizing to total protein content. N=4-7 samples/group. Note that Complex II assays were performed upon total mitochondrial lysates as *in situ* gel-based assays proved unreliable(1,2).

Supplemental Figure S3. Low-magnification transmission electron micrographs of WT and KO livers (L) and HBs (T). *A*, Representative photos (magnification x 10,000) emphasizing the relative paucity of mitochondria (white arrows) in HBs. *B*, Quantification of mitochondrial

number and size in WT livers and tumors.

Supplemental Figure S4. RNA seq analysis of differential gene expression in WT and KO HBs. Red=up-regulated; green=down-regulated. The transcripts depicted here represent all those identified with $q < 0.05$ after correction for false discovery rates.

Supplemental Figure S5. Transcripts encoding RPs. The depicted heat map is same as shown in Figure 3B. Absolute levels of expression are included.

Supplemental Figure S6. Transcripts encoding proteins involved in the regulation of translation. The depicted heat map is the same as shown in Figure 3A and includes members involved in signaling by eIF2, eIF4, p70S6K and mTOR(3,4). Absolute levels of expression are indicated thus permitting a direct comparison of transcript level differences among WT and KO hepatocytes and HBs. Note the ~11-25-fold down-regulation in both WT and KO HBs of transcripts encoding eIF4EBP3, a negative regulator of pre-initiation complex formation.

Supplemental Figure S7. Transcripts encoding glycolytic enzymes. A, The depicted heat map is the same as shown in Fig. 3C. Absolute levels of expression are included. B, The glycolytic pathway depicting key enzymes encoded by transcripts listed in A.

Supplemental Figure S8. IPA of the top categories of transcript variation between WT and KO HBs. We have previously shown that several of these pathways, which regulate functions associated with white blood cells, including “granulocyte adhesion and diapedesis” and “leukocyte extravasation signaling” are likely to be up-regulated in KO livers in response to the accumulation of lipids by hepatocytes (1). Excluding these and the already discussed pathways pertaining to protein translation, 8 of the remaining pathways (asterisks) were associated with lipid, sterol and eicosanoid biosynthesis.

Supplemental Figure S9. Differential expression of transcripts related to fatty acid biosynthesis. The data are taken from the heat map depicted in Figure 4A with actual levels of expression indicated. ND=not detected.

Supplemental Figure S10. Differential expression of transcripts related to FAO. The data are taken from the heat map depicted in Figure 4B with actual levels of expression indicated

Supplemental Figure S11. Differential expression of transcripts related to cholesterol biosynthesis. The data are taken from the heat map depicted in Figure 4C with actual levels of expression indicated.

Supplemental Figure S12. Reduced conversion of glutamine to α -ketoglutarate. A, In the liver Slc1A5 is the major glutamine transporter, whereas Gls2 and Glud1 catalyze the sequential two step deamination of glutamine to α -ketoglutarate. Glud1 also catalyzes the conversion of oxaloacetate and pyruvate to α -ketoglutarate via the actions of Got1/2 and Gpt, respectively. B, Transcript levels encoding each of the above-mentioned enzymes in WT and KO livers and HBs. Each bar represents the mean of five individual RNAseq results +/- 1 S.E. C, Immunoblots for Gls2 and Glud1 in WT and KO livers and HBs. D, The conversion of glutamine to α -ketoglutarate via the actions of Gls2 and Glud1. Each result was normalized to equivalent protein concentrations.

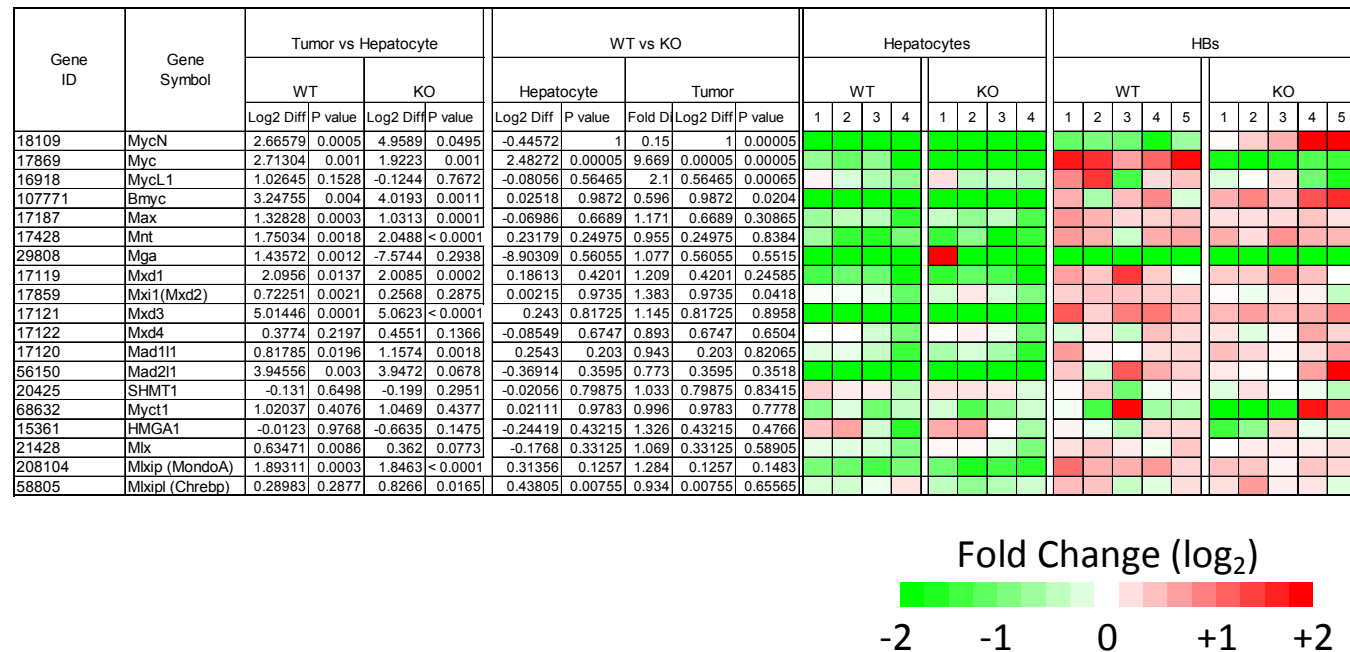
1. Edmunds, L. R., Otero, P. A., Sharma, L., D'Souza, S., Dolezal, J. M., David, S., Lu, J., Lamm, L., Basantani, M., Zhang, P., Sipula, I. J., Li, L., Zeng, X., Ding, Y., Ding, F., Beck, M. E., Vockley, J., Monga, S. P., Kershaw, E. E., O'Doherty, R. M., Kratz, L. E., Yates, N. A., Goetzman, E. P., Scott, D., Duncan, A. W., and Prochownik, E. V. (2016) Abnormal lipid processing but normal long-term repopulation potential of myc-/- hepatocytes. *Oncotarget* **7**, 30379-30395
2. Edmunds, L. R., Sharma, L., Wang, H., Kang, A., d'Souza, S., Lu, J., McLaughlin, M., Dolezal, J. M., Gao, X., Weintraub, S. T., Ding, Y., Zeng, X., Yates, N., and Prochownik, E. V. (2015) c-Myc and AMPK Control Cellular Energy Levels by Cooperatively Regulating Mitochondrial Structure and Function. *PLoS One* **10**, e0134049
3. Klann, E., and Dever, T. E. (2004) Biochemical mechanisms for translational regulation in synaptic plasticity. *Nat. Rev. Neurosci.* **5**, 931-942
4. Livingstone, M., Atas, E., Meller, A., and Sonenberg, N. (2010) Mechanisms governing the control of mRNA translation. *Phys. Biol.* **7**, 021001

Supplemental Table S1. Antibodies utilized in the current study

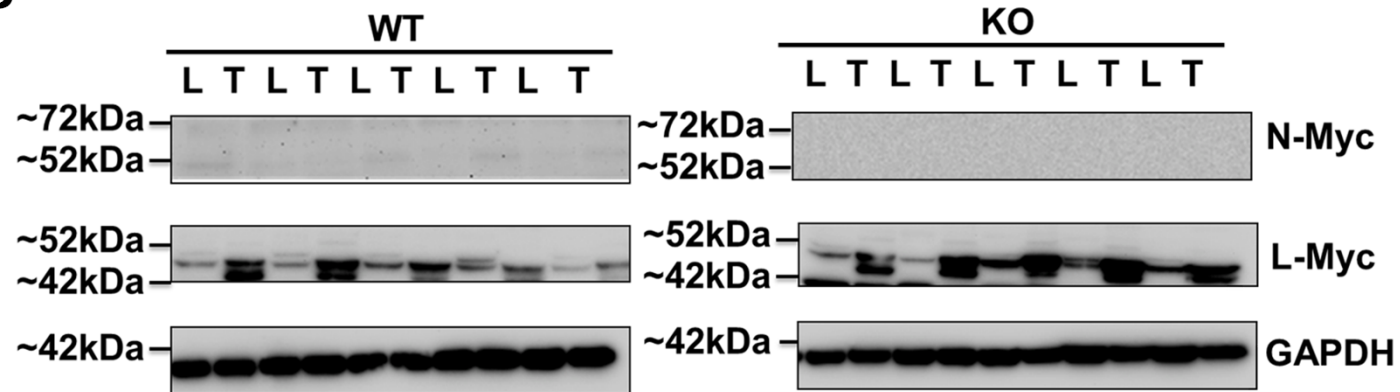
Antibody	Species	Vendor and ID no.	Dilution used
Myc	Rabbit	Cell Signaling(13987)	1:1,000
N-Myc	Rabbit	Santa Cruze(sc791)	1:500
L-Myc	Rabbit	Santa Cruze(sc790)	1:1,000
AMPK	Rabbit	Cell Signaling (3532)	1:1,000
pAMPK (Thr172)	Rabbit	Cell Signaling (4188)	1:1,000
Histone H3	Rabbit	Cell Signaling (9715)	1:1,000
Glutaminase 2	Rabbit	Abcam(ab113509)	1:1,000
Glutamine dehydrogenase	Rabbit	Cell signaling(12793)	1:1,000
Acetyl-histone-H3 (K9/K14)	Rabbit	Santa Cruz (sc8655-R)	1:500
GAPDH	Mouse	Sigma-Aldrich(G8795)	1:20,000
HRP anti-mouse	Horse	Cell Signaling(7076)	1:10,000
HRP anti-rabbit	Goat	Cell Signaling(7074)	1:5,000
Alexa Fluor 488 anti-rabbit	Goat	Thermo Fisher(A-11008)	1:1,000

Supplemental Fig. S1

A

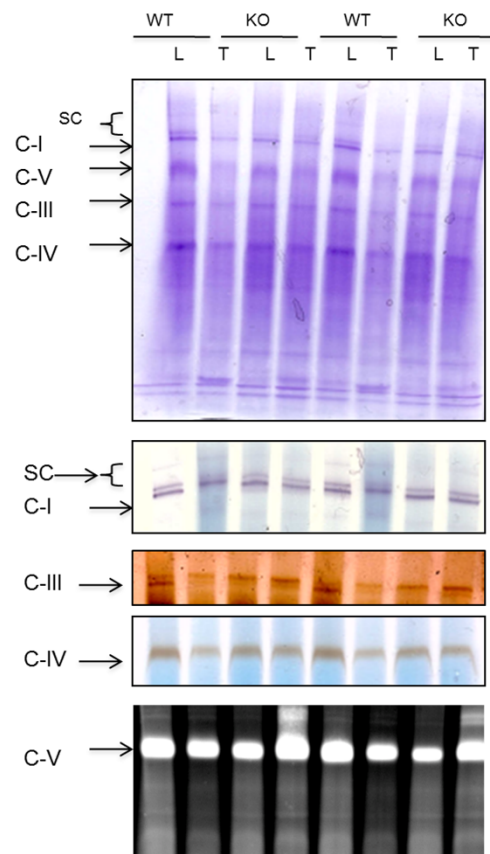


B

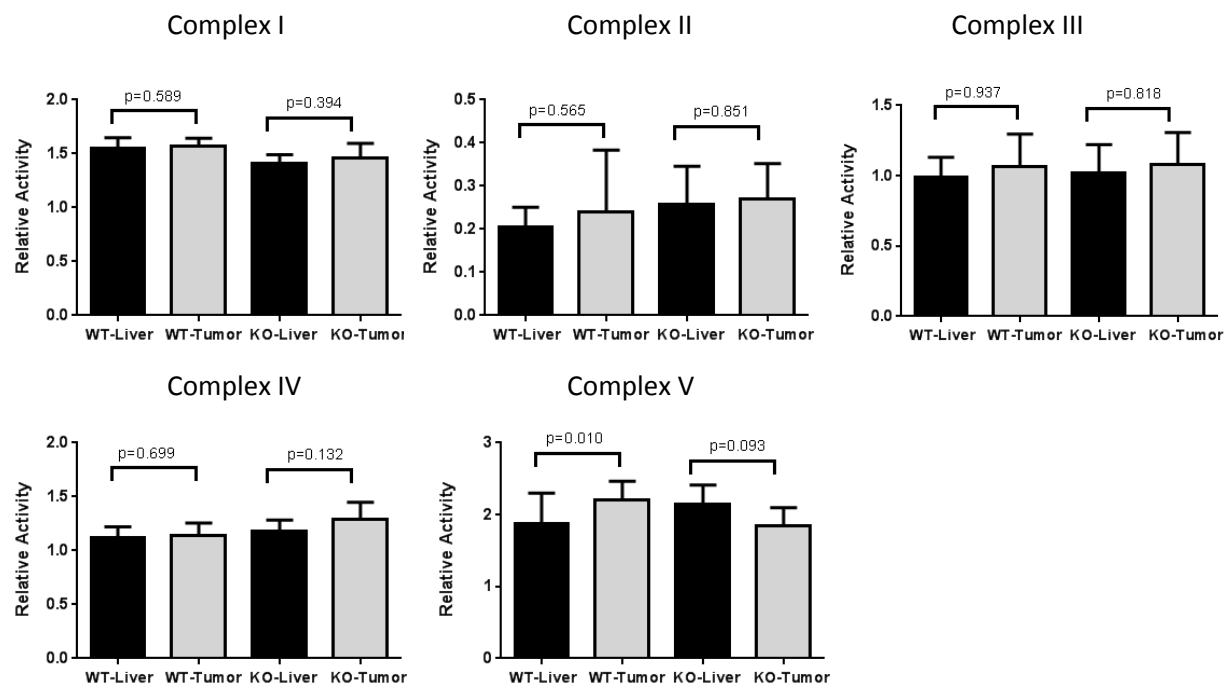


Supplemental Fig. S2

A

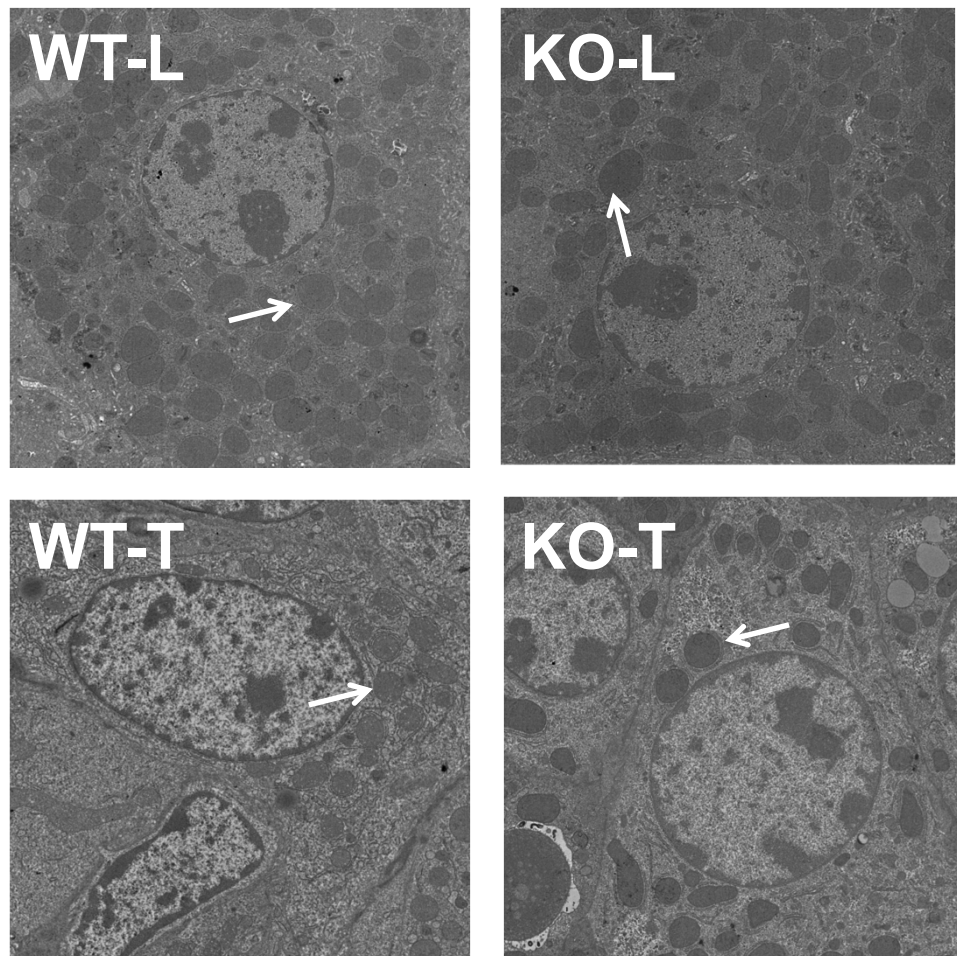


B

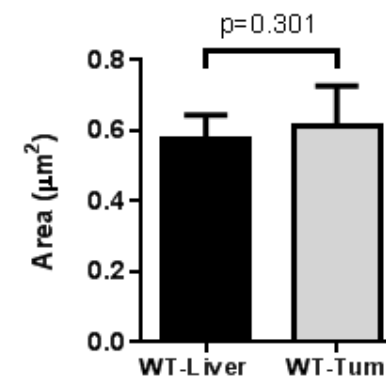
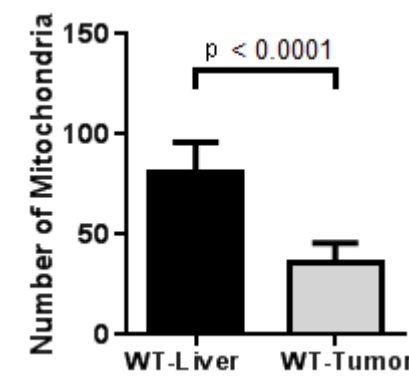


Supplemental Fig. S3

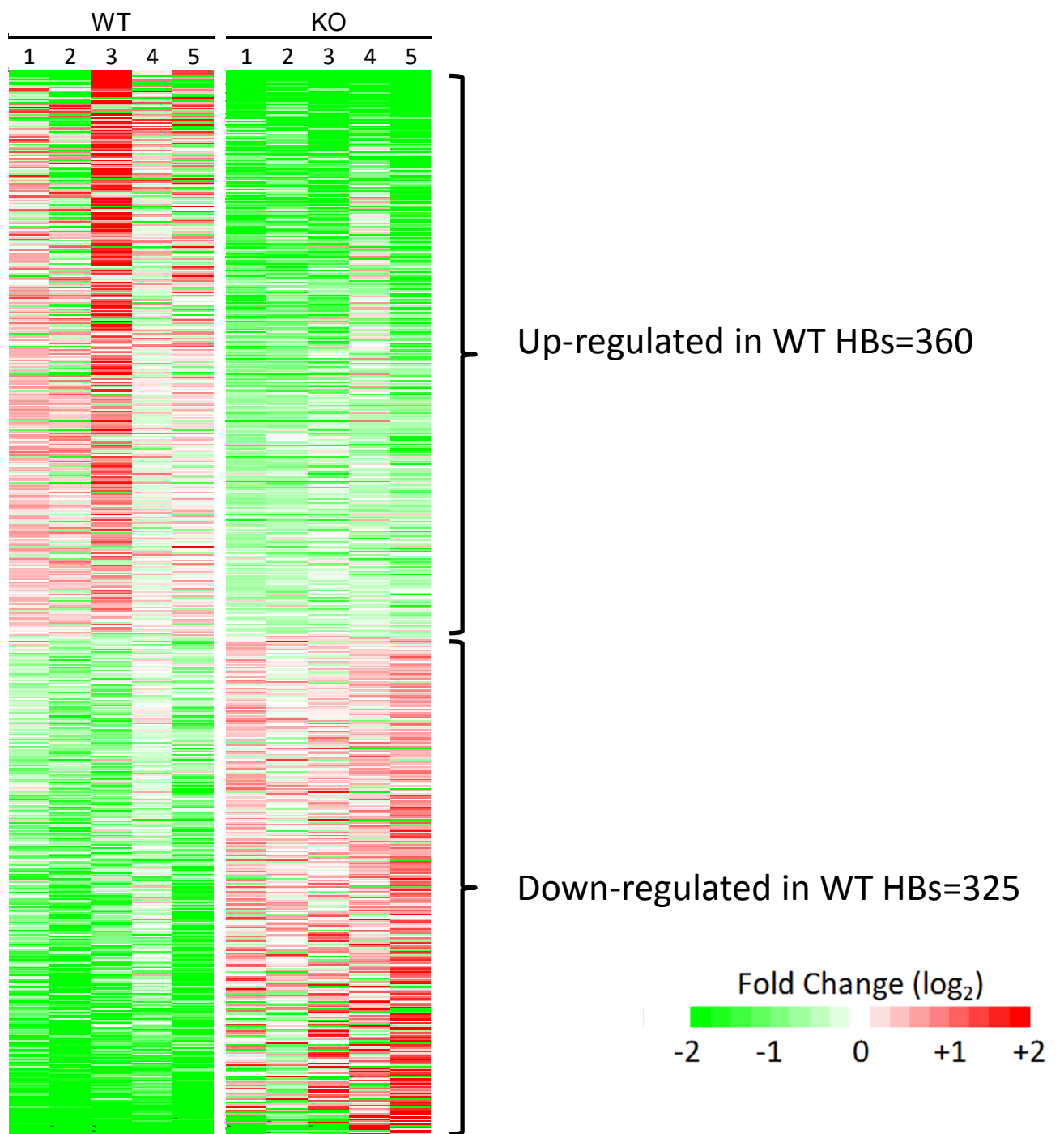
A



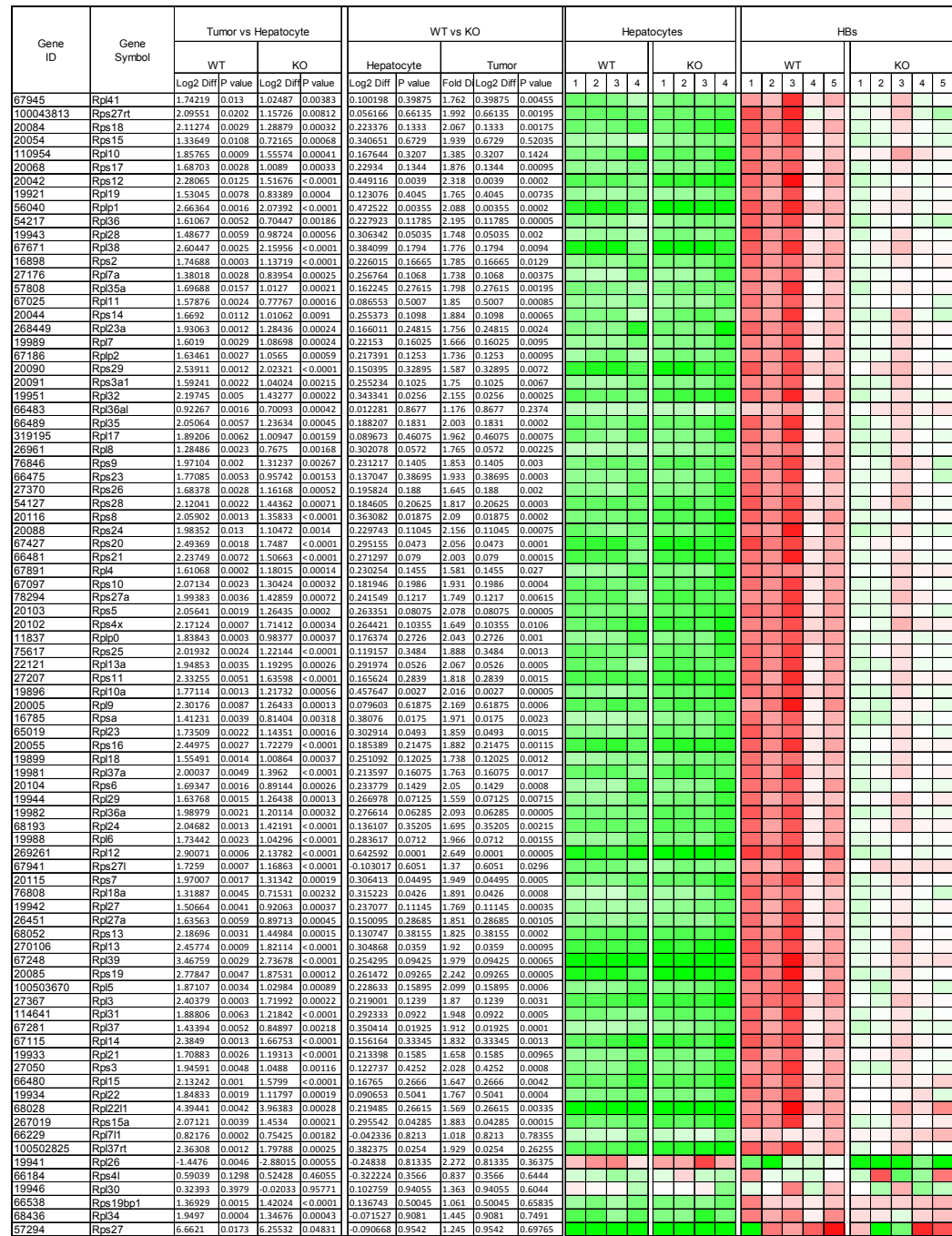
B



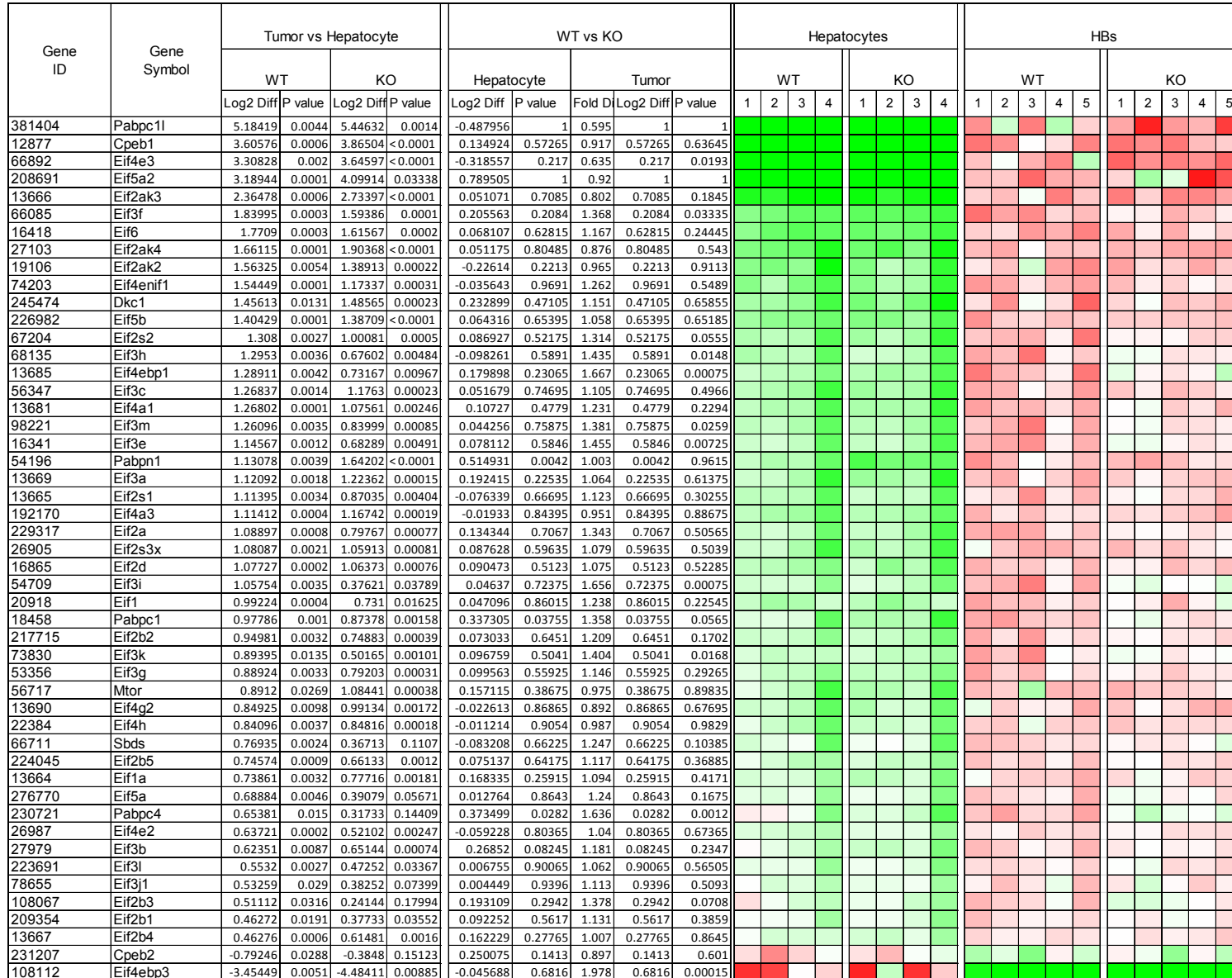
Supplemental Fig. S4



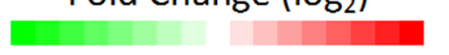
Supplemental Fig. S5



Supplemental Fig. S6

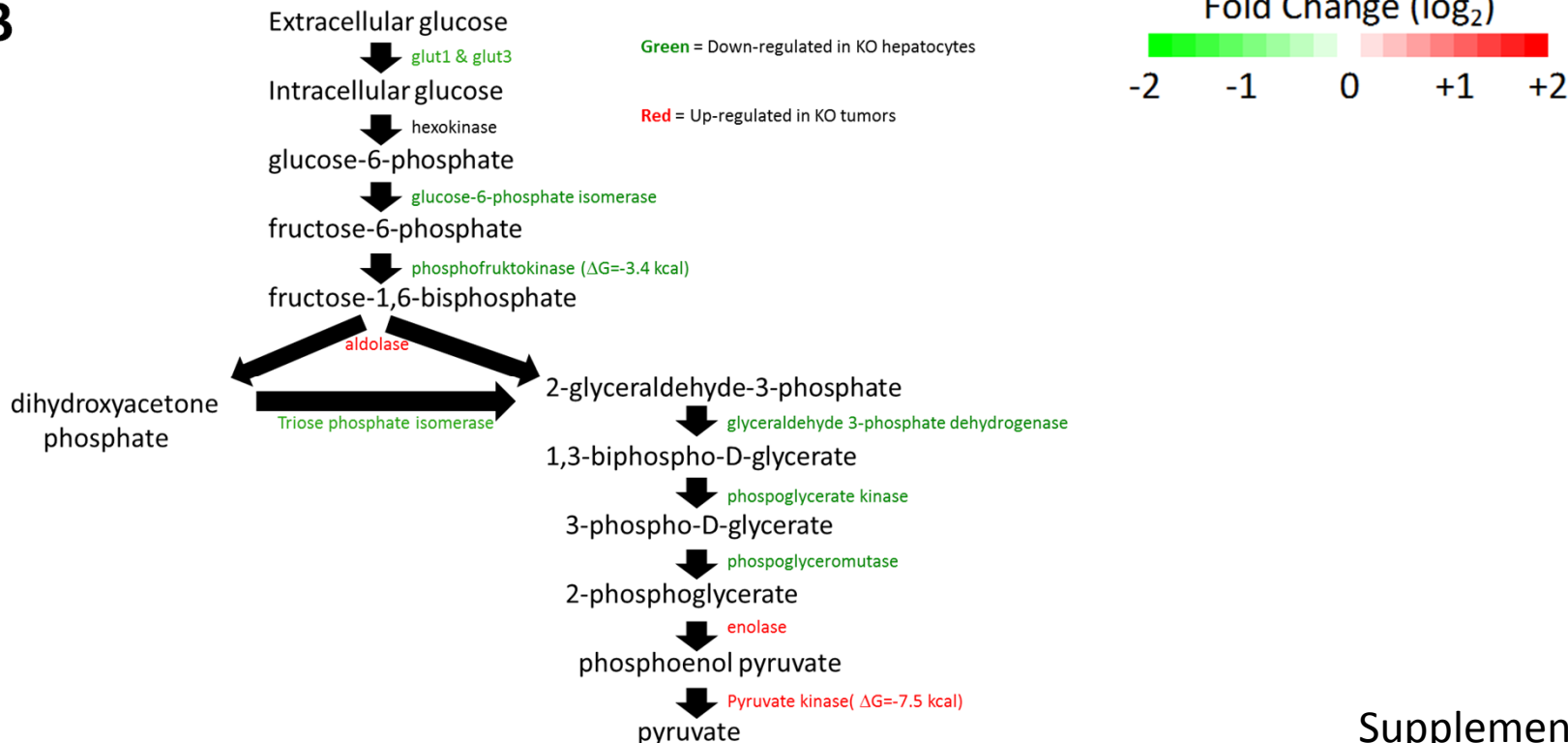


Fold Change (\log_2)

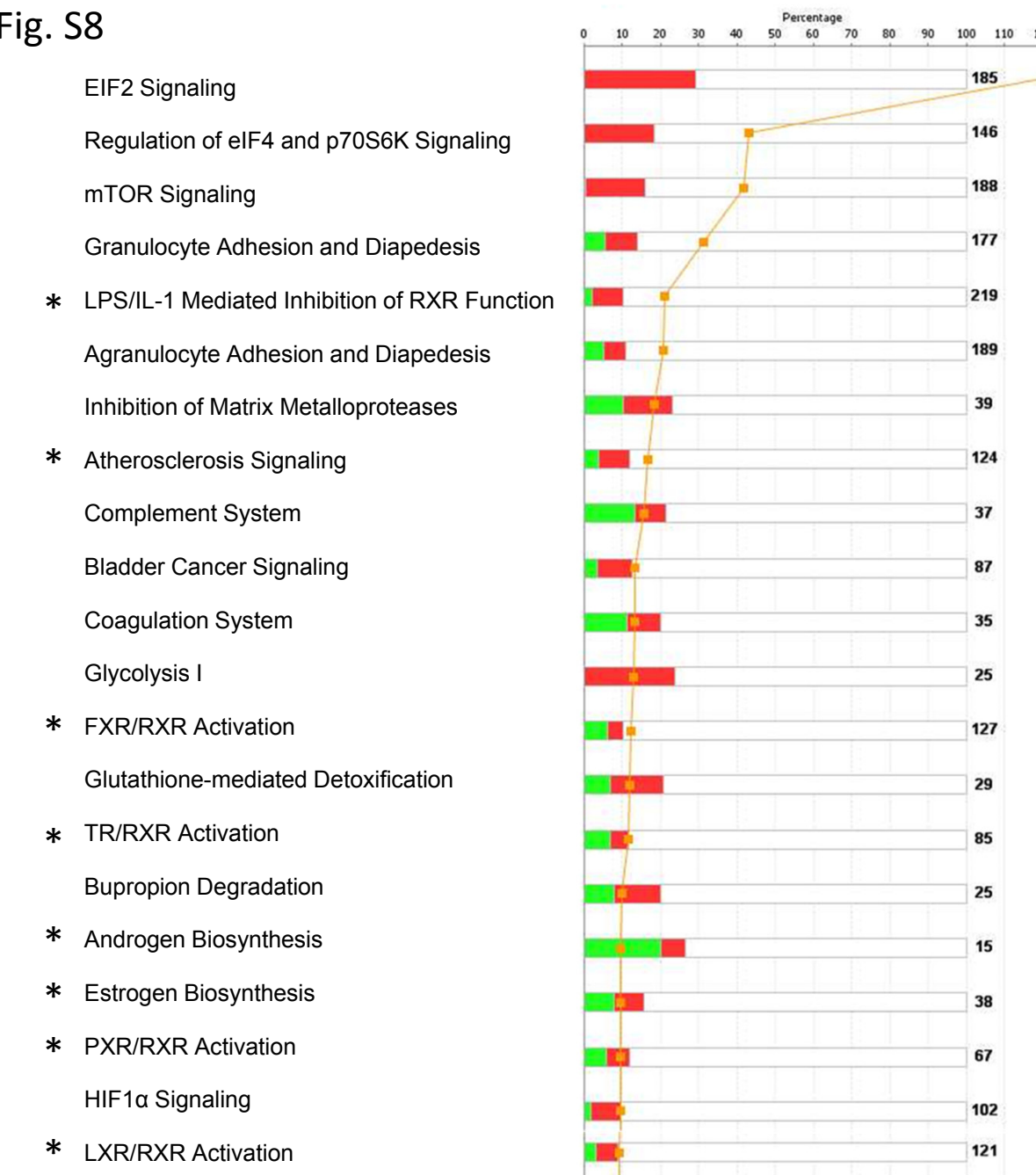


A

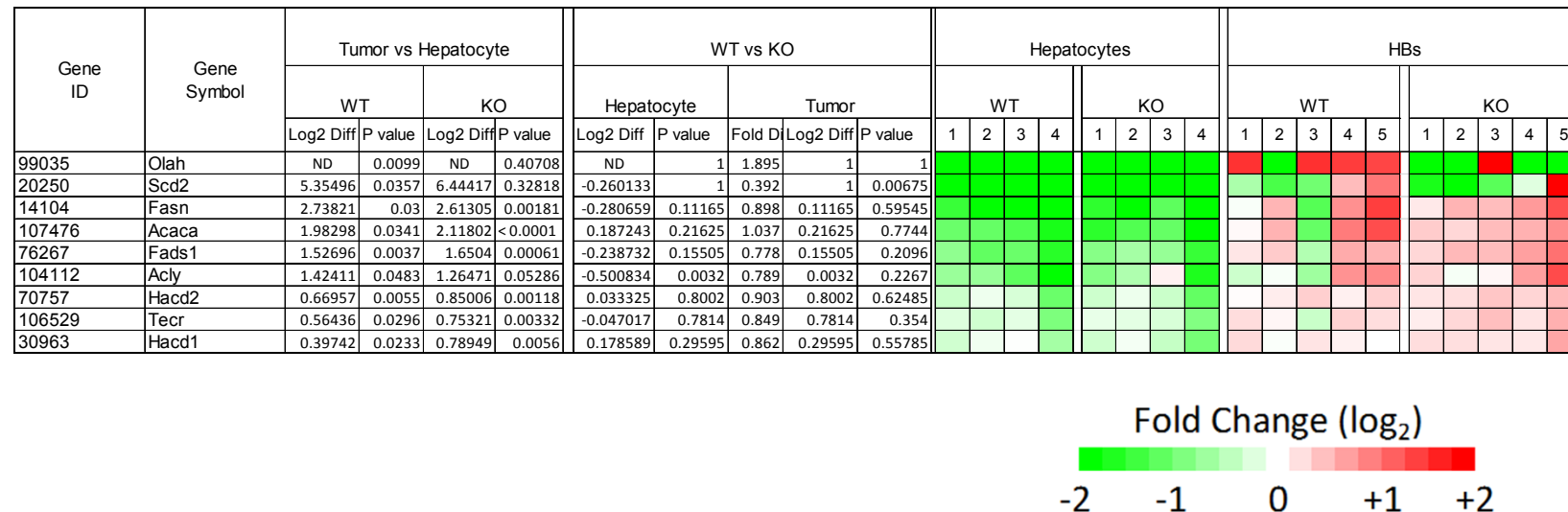
Gene ID	Gene Symbol	Tumor vs Hepatocyte				WT vs KO				Hepatocytes				HBs										
		WT		KO		Hepatocyte		Tumor		WT		KO		WT		KO								
		Log2 Diff	P value	Log2 Diff	P value	Log2 Diff	P value	Fold D	Log2 Diff	P value	1	2	3	4	1	2	3	4	5	1	2	3	4	5
20525	SLC2A1	1.58506	0.1198	0.47423	0.19863	0.20369	0.1633	2.487	0.1633	0.00005														
20526	SLC2A2	1.31565	0.0258	0.51479	0.12053	-0.524995	0.0025	1.211	0.0025	0.22935														
20527	SLC2A3	4.85613	0.1233	4.83753	0.00706	1.387674	1	2.651	1	0.00805														
20528	SLC2A4	6.07493	0.0198	6.56371	<0.0001	0.619948	1	1.095	1	0.78														
15275	HK1	3.63795	0.0783	2.5991	0.02999	-0.191743	1	1.799	1	0.02255														
15277	HK2	5.75422	0.045	4.49358	0.00307	-0.606021	1	1.574	1	0.0651														
212032	HK3	3.03876	0.0134	3.53789	0.01232	0.679162	1	1.133	1	0.5318														
14751	GPI1	1.46372	0.0015	0.71571	0.00077	0.150086	0.30745	1.864	0.30745	0.0002														
18641	PFKL	2.57103	0.0066	2.04986	<0.0001	0.131595	0.50285	1.572	0.50285	0.0022														
18642	PFKM	0.15914	0.5869	0.505	0.03512	0.219948	0.3057	0.916	0.3057	0.7656														
56421	PFKP	4.07116	0.0243	3.0525	0.00121	-0.121706	1	1.862	1	0.1705														
11674	ALDOA	1.84761	0.0628	0.54645	0.00773	0.121555	0.3214	2.681	0.3214	0.00005														
230163	ALDOB	-1.16576	0.002	-1.51574	0.00099	-0.20247	0.47945	1.108	0.47945	0.6644														
11676	ALDOC	3.64566	0.0012	2.65665	<0.0001	-0.552653	0.019	1.353	0.019	0.05335														
14433	GAPDH	-0.04584	0.8477	-0.72266	0.0124	-0.019563	0.9564	1.577	0.9564	0.0145														
14447	GAPDHS	3.1865	0.0059	3.77327	0.00029	0.976888	1	1.31	1	0.4964														
18655	PGK1	0.47065	0.2311	-0.47368	0.02162	-0.053085	0.7048	1.855	0.7048	0.0003														
12183	BPGM	0.02313	0.8975	-0.0589	0.72372	0.06457	0.77035	1.107	0.77035	0.4815														
18648	PGAM1	0.77814	0.0288	0.2355	0.26493	0.063955	0.6586	1.523	0.6586	0.0077														
13806	ENO1	0.07807	0.853	-0.592	0.11035	-0.079343	0.75145	1.506	0.75145	0.1079														
433182	ENO1B	1.79967	0.0014	1.13356	0.00137	0.009521	0.81115	1.597	0.81115	0.22245														
13808	ENO3	1.17718	0.0213	1.61451	0.00492	0.702704	0.0042	1.202	0.0042	0.40945														
18770	PKLR	1.78039	0.0679	1.09927	0.00254	-0.428274	0.00815	1.192	0.00815	0.2756														
18746	PKM	5.48674	0.0598	3.72967	0.00661	0.029697	0.9775	3.45	0.9775	0.00005														
18597	PDHA1	0.32312	0.1644	0.158	0.46156	0.036679	0.77515	1.15	0.77515	0.29025														
68263	PDHB	-0.13949	0.49	-0.29326	0.14184	-0.059054	0.7536	1.068	0.7536	0.5415														

B

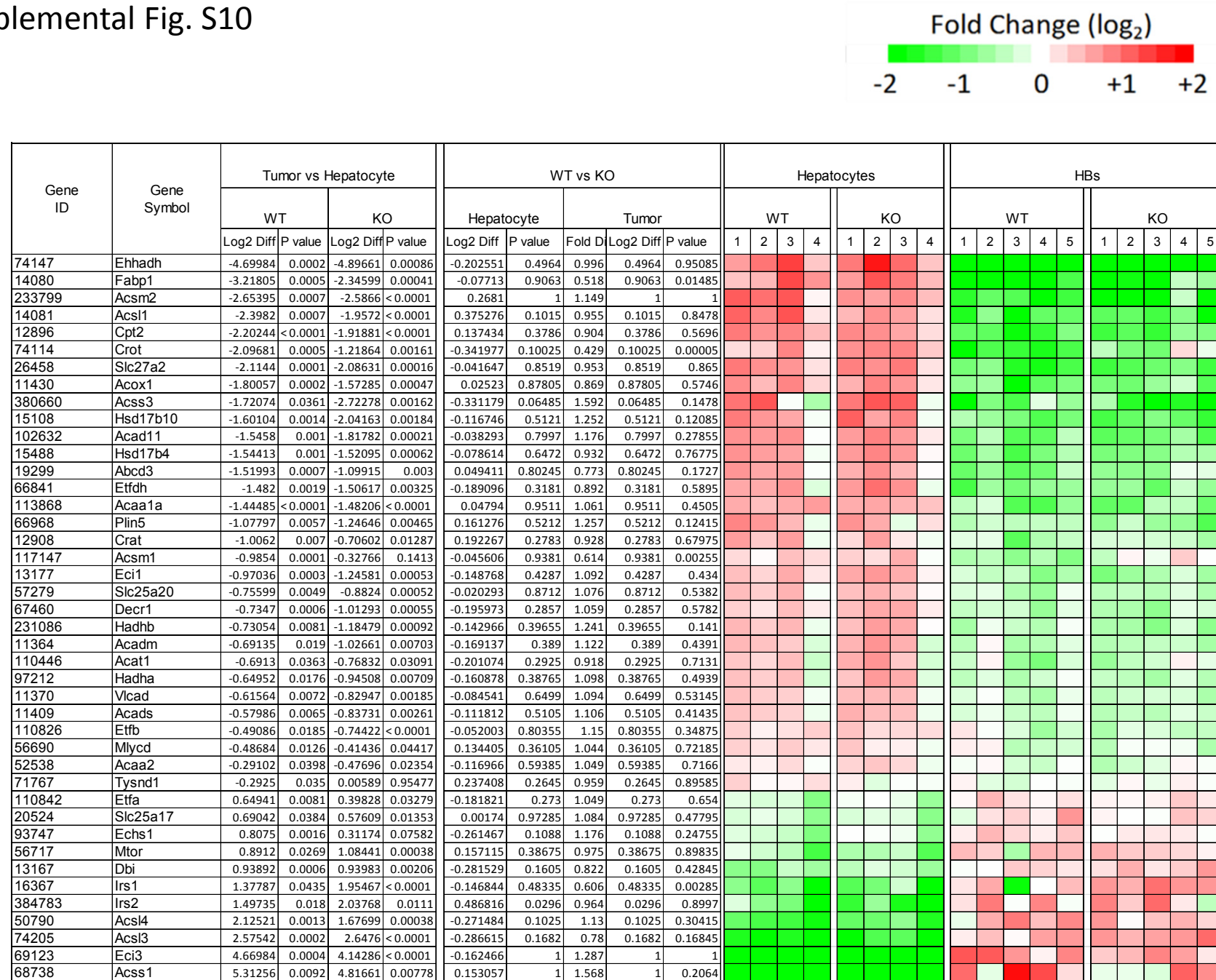
Supplemental Fig. S8



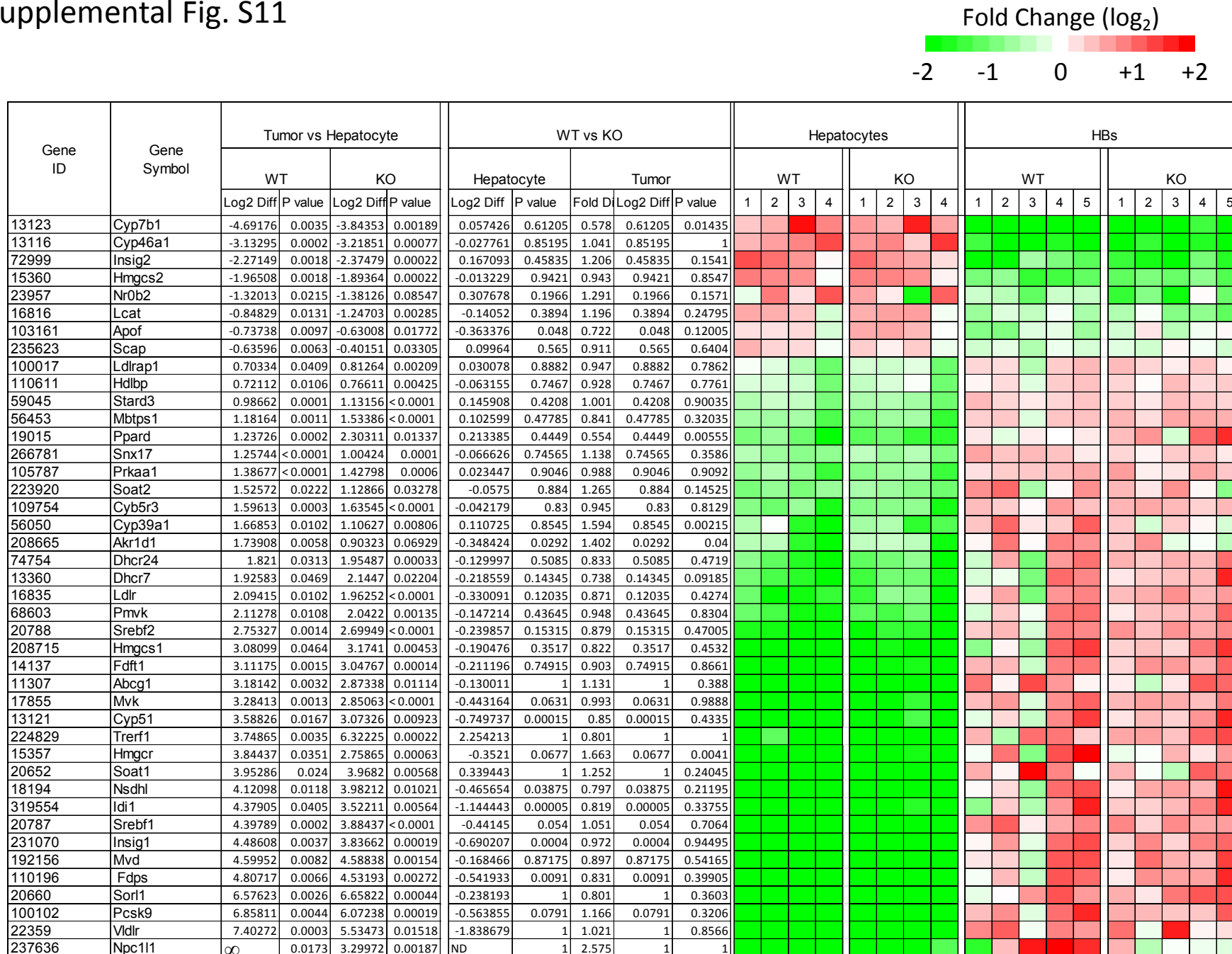
Supplemental Fig.S9



Supplemental Fig. S10

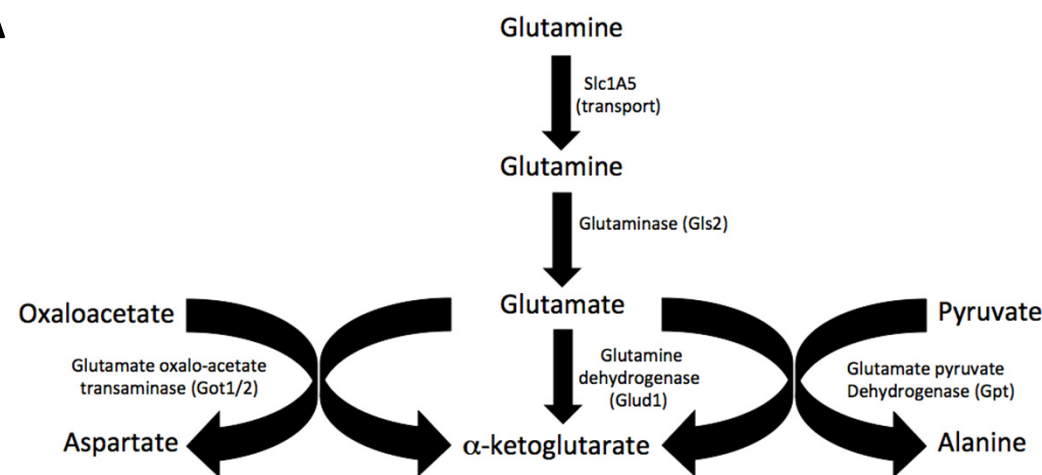


Supplemental Fig. S11

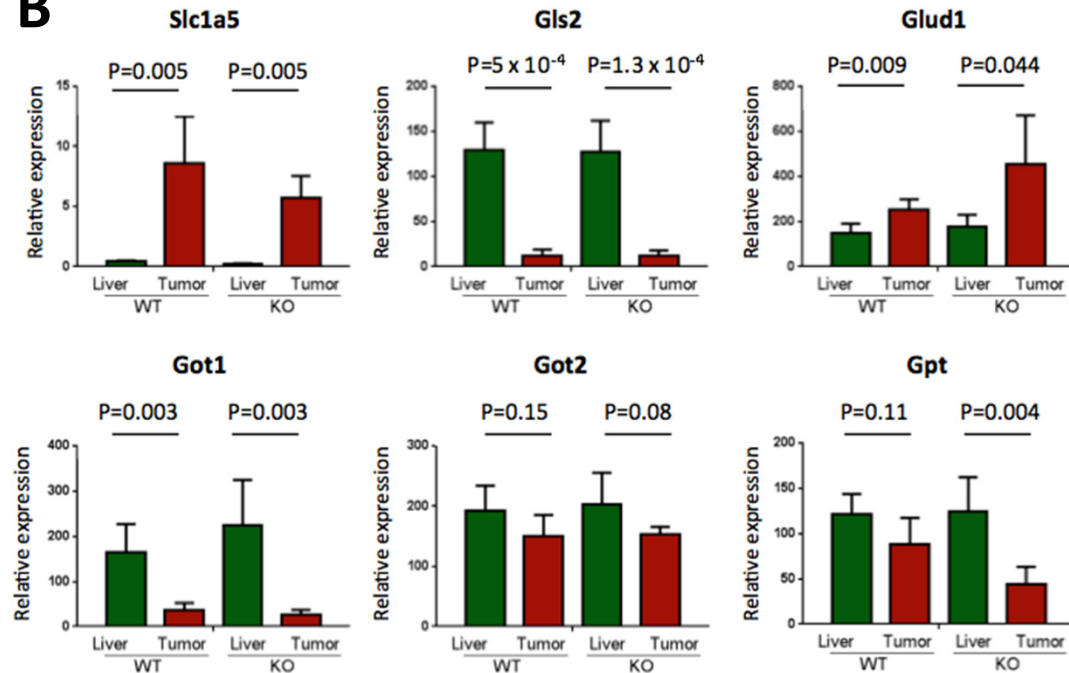


Supplemental Fig. S12

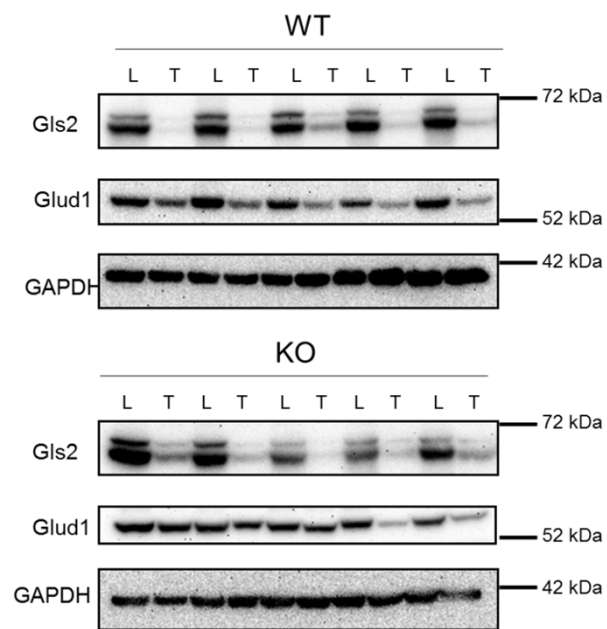
A



B



C



D

